ELSEVIER

Thermochimica Acta 291 (1997) 85–94

thermochimica acta

Modulated differential scanning calorimetry in the glass transition region, IV.[1] Pseudo-isothermal analysis of the polystyrene glass transition[2]

Leonard C. Thomas[a], Andreas Boller[b], Iwao Okazaki[3,b], Bernhard Wunderlich[b,*]

[a] *TA Instruments, Inc. 109 Lukens Drive, New Castle, DE 19720, USA*

[b] *Department of Chemistry, The University of Tennessee, Knoxville, TN 37996-1600, and the Chemistry and Analytical Sciences Division, Oak Ridge National Laboratory, Oak Ridge, TN 37831-6197, USA*

Received 4 April 1996; received in revised form 24 June 1996; accepted 29 July 1996

Abstract

The kinetics of the glass transition of Polystyrene is measured by quasi-isothermal, temperature-modulated differential scanning calorimetry (TMDSC) and compared to pseudo-isothermal analyses of standard TMDSC traces. Quasi-isothermal TMDSC is carried out at a series of fixed average temperatures, modulated sinusoidally with an amplitude of ±1.0 K and a period of 100 s. These measurements use, thus only a single time scale defined by the modulation frequency. The standard use of TMDSC adds a second time scale to the experiment, the underlying heating and cooling rates $\langle q \rangle$ at 1 K min^{-1}. In the pseudo-isothermal analysis of standard MDSC, the effects of the underlying heating and cooling rates are separated by subtraction of averages over full modulation periods from the modulated temperature and heat flow. The small differences in the reversing, apparent heat capacity between MDSC heating and cooling traces are measured and linked to the kinetic expressions of irreversible thermodynamics and interpreted using the hole theory. As the sample moves away from the equilibrium of the liquid state, the kinetics depends increasingly on the thermal history, and the expected deviations from a first-order kinetic expression are observed. © 1997 Elsevier Science B.V.

Keywords: Temperature modulated calorimetry; Heat capacity; Glass transition; Irreversible thermodynamics; Polystyrene

1. Introduction

Temperature-modulated differential scanning calorimetry (TMDSC) has become a well-established new measurement technique permitting the evaluation of time-dependent processes via irreversible thermodynamics. The commercially available modulated differential scanning calorimeter (MDSC) permits a separation of nonreversing processes from reversing ones [1]. In MDSC, a sample is heated with an underlying rate $\langle q \rangle$ that is modulated by a sinusoidally changing temperature, leading to a sample temperature, $T_s = T_o + \langle q \rangle t + A \sin \omega t$, where T_o is the starting temperature; t, the time; A, the maximum modulation amplitude; and ω, the modulation frequency ($=2\pi/p$, with p being the modulation period). The response to the heating program is seen in the temporal change of the temperature difference between symmetrically

*Corresponding author. Tel.: 423 974 0652 and 423 574 8741; fax: 423 974 3419 or 423 974 3454; e-mail: athas@utk.edu.

[1] Presented in part at the 24th Conference of the North American Thermal Analysis Society, San Francisco, CA, September 10–13, 1995.

[2] The submitted manuscript has been authored by a contractor of the US Government under the contract No. DE-AC05-96OR22464. Accordingly, the US Government retains a non-exclusive, royalty-free license to publish, or reproduce the published form of this contribution, or allow others to do so, for US Government purposes."

[3] On leave from Toray Industries, Inc. Otsu, Shiga 520, Japan.

PII S0040-6031(96)03071-7

placed reference and sample calorimeters. This temperature difference $\Delta T=T_r-T_s$ is proportional to the heat flow, HF. The sinusoidal part of the response is then separated mathematically from the temperature and temperature difference signals and used to compute the reversing part of the measurement (pseudo-isothermal analysis) [2]. The calorimetric signal at time t, HF(t), when averaged over an integral period of the modulation ($t\pm 1/2p$), in turn, is taken as a measure of the total differential heat flux, $\langle HF(t)\rangle$. While the pseudo-isothermal response is governed by the modulation frequency, $\langle HF(t)\rangle$ should be governed, as in standard DSC, by the underlying heating and cooling rates $\langle q\rangle$. In the glass transition region this separation is only approximate, as will be shown in this paper. The MDSC analysis involves, thus, two different time scales in the same experiment. Only if the thermal response of the sample is time independent, one can expect the same result from the reversing and total signals and, in turn, from MDSC and traditional DSC.

This ability to measure a time-dependent response is of special importance for the analysis of the glass transition. Depending on the thermal history, glasses have different levels of stability, measurable by the level of enthalpy, H, and Gibbs function, G. Both are linked to the heat capacity, measurable by calorimetry [$(dH/dT)=C_p$, and $(d^2G/dT^2)=-C_p/T$]. Traditional DSC with a fixed heating rate leads already to complications in the glass transition region. One obtains glasses of increased stability (lesser H and G) when cooling with slower cooling rates through the glass transition, or when annealing for longer times below the glass transition temperature, T_g. Different DSC traces are observed on heating of such glasses with different thermal histories at the same heating rate, or on heating a glass with a given thermal history with different heating rates. An effort has been made some time ago to explain the different DSC traces by using the simple, first-order kinetics model of irreversible thermodynamics, linked to the hole model of the glass transition [3]. It is the aim of this paper to resolve some of the even more complicated traces that result by adding modulation to the standard DSC experiment.

This is the fourth of a series of papers on the analysis of the glass transition. The first paper describes the general separation of the enthalpy relaxation from the reversing heat capacity signal [4]. It is shown there, that even in the presence of a large enthalpy relaxation, MDSC can establish a frequency-dependent glass transition temperature on heating. The pseudo-isothermal separation of the reversing heat capacity on heating and cooling leads to approximately equal values. The remaining inequality is discussed in this paper. For glasses with different stability, a small difference in C_p was found in the low-temperature region of the glass transition, that will be of importance for the present discussion and further work on partially crystalline materials [5]. The first paper in this series indicated also that more precise data can be obtained by measuring quasi-isothermally (i.e. using a $\langle q\rangle$ of zero at a series of constant temperatures in the glass transition region [6]). The mathematical treatment of the quasi-isothermal MDSC in the glass transition region is described in Part II of this series [7]. The third part, finally, showed a quantitative analysis of the glass transition of polystyrene and poly(ethylene terephthalate) [8]. The MDSC response was, next, further evaluated with a modeling approach that duplicates the MDSC software using a spread-sheet analysis [9]. This spread-sheet computation is used in the present analysis to compare the kinetics computations to the experimental data.

2. Experimental conditions and results

2.1. Instrumental details

A commercial Thermal Analyst 2920 system from TA Instruments with modulated DSC (MDSC) was used for all measurements. Helium gas with flow rate of 30 $cm^3\ min^{-1}$ was purged through the cell. Cold nitrogen, generated from liquid nitrogen was used for cooling. The sample mass was 9.51 mg. For calibration of the heat flow amplitude sapphire was used. The pan weights were always about 23 mg and matched on the sample and reference sides. Detailed graphs of the limits of modulation as a function of temperature and cooling capacity were published earlier [6]. Also, a discussion of steady state under such measuring conditions has been given [10]. In the present experiments, steady state is estimated to be within $\approx 1\%$ of the change in heat capacity.

Two kinds of experiments have been carried out. First, to see the effect of the underlying heating and cooling rates, a series of continuous MDSC runs were done at $\langle q \rangle = \pm 1$ K min^{-1}. Three heating and two cooling experiments were carried out in sequence with the same sample. The modulation period p was 100 s and the amplitude was set to $A = 1.0$ K (maximum additional q due to modulation $= \pm 3.77$ K min^{-1}). The standard MDSC for pseudo-isothermal analysis was compared to the second set of measurements, carried out quasi-isothermally in 1 K steps. One set of measurements started at 360 K, the other at 390 K, to cover the glass transition region from both directions of temperature.

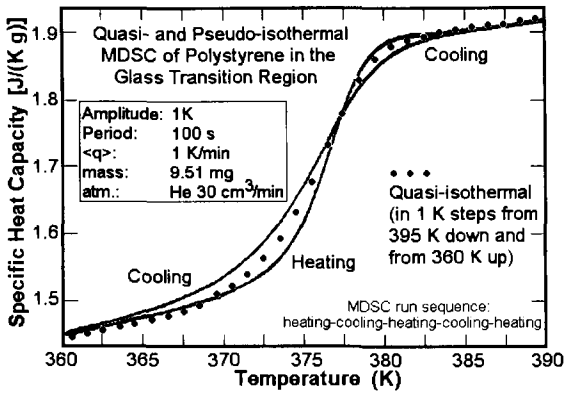

Fig. 1. Experimental data (total specific heat capacity, vibrational and "hole" contribution, as given in Eq. (1)).

2.2. Data treatment and results

The recording and deconvolution of the signals was done by the software of the chosen MDSC, using the earlier detailed method [6]. The reversing heat capacity is extracted from the modulation amplitudes and given, for the case of equal mass of the empty sample and reference pans, by:

$$mc_p = \frac{A_\Delta}{A}\sqrt{\left(\frac{K}{\omega}\right)^2 + C'^2} \tag{1}$$

with C' representing the pan heat capacity; K, the Newton's law constant of the calorimeter; c_p, the specific heat capacity of the sample; m, the sample mass; and A_Δ, the modulation amplitude of the temperature difference ΔT (A_Δ is proportional to the heat flow amplitude A_{HF}).

Fig. 1 shows the results for 65 experiments (5 standard MDSC traces evaluated pseudo-isothermally and 60 quasi-isothermal measurements). The quality of the measurement can also be judged from the figure. Differences of the repeat DSC traces are hardly visible and the quasi-isothermal data-points on heating and cooling lie within the margins of the filled circles.

The heat capacity computed with the MDSC software is equal to:

$$mc_p = K_C \times \frac{\text{smoothed}\langle A_{HF}\rangle}{\text{smoothed}\langle A\rangle} \times \frac{1}{\omega} \tag{2}$$

where K_C is the heat capacity calibration constant, fitted to data from runs with sapphire [11] at the given temperature, frequency, and pan weights, and is given by:

$$K_C = C_p(Al_2O_3, \text{literature}) \times \frac{\text{smoothed}\langle A\rangle}{\text{smoothed}\langle A_{HF}\rangle} \times \omega \tag{3}$$

with A and A_{HF} in Eq. (3) representing the calibration run. For the present research the enthalpy relaxation, or hysteresis effects, that show mainly in the total and nonreversing heat flows of the experiment, were not further analyzed.

2.3. Samples

The sapphire disc and indium for amplitude and temperature calibration, respectively, were supplied with the accessory kit of the MDSC instrument. A standard ICTAC sample of polystyrene was used for the research. The heat capacity of such standard polystyrene is available in the ATHAS data bank for comparison [12], and the glass transition for GM-754 was reported to be 378 K (heating rate 10 K min^{-1}). The quasi-isothermal data of Fig. 1 were analyzed as described before [8] and give an activation energy of $\varepsilon_j = 499.1$ kJ mol^{-1} and a pre-exponential factor $B = 2.932 \times 10^{-68}$ s for the temperature dependence of the relaxation time τ, to be used in Eq. (8). Both measurements at increasing and decreasing temperature are represented with the same parameters. It should be noted that the standard sample is different

from the polystyrene analyzed in Ref. [8]. The latter has a lower glass transition temperature and activation energy. The rather large changes of activation energy and pre-exponential factors that are caused by prior sample treatment are discussed in more detail on the example of poly(ethylene terephthalate) [5]. Changes of similar magnitude are expected from differences in synthesis and processing.

3. Description of the glass transition kinetics

Below the glass transition temperature, T_g, the heat capacity C_p consists practically only of vibrational contributions, C_{p_o}, and is virtually time-independent:

$$C_p(\text{solid}) = C_{p_o}. \tag{4}$$

In the liquid state, longer times are necessary to reach thermal equilibrium because of the need of the molecules to undergo additional, cooperative, structure changes. In the glass transition region, both liquid and solid heat capacities are available by extrapolation from measurements outside the glass transition region. A simple mechanistic model for the representation of the liquid heat capacity has been given by Eyring and Frenkel in terms of a hole theory [13], i.e. the larger expansivity of liquids and the slower response to external forces is taken to be due to a temperature-dependent equilibrium of collapse and formation of holes of equal sizes. The equilibrium number of the holes is N^*, and each mole of holes contributes an energy ε_h to the enthalpy (heat of formation). The hole contribution to the heat capacity is then given by the change in number of holes with temperature under equilibrium conditions [3]. The total heat capacity in equilibrium is:

$$C_p(\text{liquid}) = C_{p_o} + \varepsilon_h\left(\frac{dN^*}{dT}\right). \tag{5}$$

For polystyrene it was found in Ref. [8] that ε_h=6.00 kJ mol^{-1} and $dN^*/dT=\alpha=5.13\times10^{-3}$ mol K^{-1}. The hole theory can be applied to the glass transition by considering the kinetics of the hole formation [14]. One can write a simple, first-order kinetic expression as results also from a description of the kinetics of the glass transition in terms of irreversible thermodynamics [5,9] and is then free of the explicit model:

$$\left(\frac{dN}{dt}\right) = \frac{1}{\tau}(N^* - N). \tag{6}$$

In Eq. (6) N represents the instantaneous number of holes or number of high-enthalpy configurations, N^* their equilibrium number, and τ the relaxation time for the formation of the extra enthalpy. In the framework of the irreversible thermodynamics $1/\tau$ is proportional to the curvature of the free enthalpy relative to N, the internal variable [15]. Eq. (6) can, next, be used to describe the apparent, time-dependent, heat capacity, $C_p^{\#}$, by replacing dN^*/dT in Eq. (5) with $dN/dT=(\partial N/\partial T)_t+(\partial N/\partial T)_T\times(dt/dT)$.

The solution of Eq. (6) was given earlier as [3]:

$$N(t) = N(t_o)\exp(-\Phi(t)) + \exp(-\Phi(t)) \times \int_{t_o}^{t} \frac{N^*(t')}{\tau(t')}\exp(\Phi(t))dt' \tag{7}$$

$$\Phi(t) = \int_{t}^{t_o} \frac{1}{\tau(t')}dt',$$

where t_o is the beginning of the experiment, and $\Phi(t)$ is the time-integrated inverse relaxation time. Both τ and N^* are to be inserted into Eq. (7) with their proper temperature and time dependence. For the limited temperature range of the glass transition region, one can assume that τ has an Arrhenius-type temperature dependence $\tau=B\exp\varepsilon_j/(RT)$. For the simpler, quasi-isothermal measurements, the solution of Eq. (7) is described in paper III of this series and a method was proposed to derive the parameters for the description of τ [8].

Extending the analysis to the case of pseudo-isothermal analysis of the MDSC experiment where $T_s=T_o+\langle q\rangle t+A\sin\omega t$, the time-dependence of τ can be written as:

$$\tau(t') = B\exp\frac{\varepsilon_j}{RT_o}\left(1+\frac{\langle q\rangle t'}{T_o}+\frac{A}{T_o}\sin\omega t'\right)^{-1}. \tag{8}$$

For the derivation of the time dependence of N and the relaxation time τ over one modulation period, two

normalized, dimensionless modulation amplitudes were introduced [8]:

$$A_N = \frac{A\alpha}{N_o^*} \quad \text{and} \quad A_\tau = \frac{A\varepsilon_j}{RT_o^2} \tag{9}$$

where A is, as before, the amplitude, set for the temperature modulation, and α is the change of N^* with temperature as contained in Eq. (5). The reference values N_o^* and T_o are taken at the midpoint of the temperature increase due to $\langle q\rangle t'$ for the modulation cycle under consideration. The two amplitudes of Eq. (9) describe the effects due to the change in N^* and the relaxation time during the modulation cycle, respectively. The effect of the underlying, linear heating rate ($\langle q\rangle$) requires two more constants of dimension 1/time:

$$q_N = \frac{\langle q\rangle\alpha}{N_o^*} \quad \text{and} \quad q_\tau = \frac{\langle q\rangle\varepsilon_j}{RT_o^2}. \tag{10}$$

As long as $(\langle q\rangle t + A\sin\omega t)/T_o$ is small relative to one, Eq. (8) can be expressed simply as:

$$\tau(t) = \tau_o(1 - q_\tau t - A_\tau \sin\omega t) \tag{11}$$

and Eq. (6) takes now the form:

$$\left(\frac{dN}{dt}\right) = \frac{N_o^*(1 + A_N \sin\omega t + q_N t) - N_o}{\tau_o(1 - q_\tau t - A_\tau \sin\omega t)}. \tag{12}$$

The solution of Eq. (12) is rather involved, especially since the experiments show that A_τ is larger than A_N, so that $\Phi(t)$ of Eq. (7) remains temperature dependent. An approximate solution of Eq. (12) reveals modulated cross-term that involve A_N, A_τ, q_N, and q_τ. This indicates that the modulation and the linear heating rate contribute to the reversing heat capacity. On heating and cooling, different reversing heat capacities are therefore expected. Rather than solving Eq. (12) approximately, it is easier to use a numerical solution for Eq. (6), as will be shown next.

4. Numerical solution for the apparent heat capacity

The numerical solution for Eq. (6) chosen for this discussion involves integration of one-second intervals with a constant N^* and an average value of τ as given by:

$$N_i = N_i^* - (N_i^* - N_{i-1})\exp\left(-\frac{t}{\sqrt{\tau_i \times \tau_{i-1}}}\right) \tag{13}$$

with i representing the running index of time. With one-second intervals $i=t$, and the complete range of the experiment is covered in 2500 steps of summation. The results for $N(t)$ and $\Delta N(t)$ are shown in Fig. 2 for cooling, and in Fig. 3 for heating. For the cooling

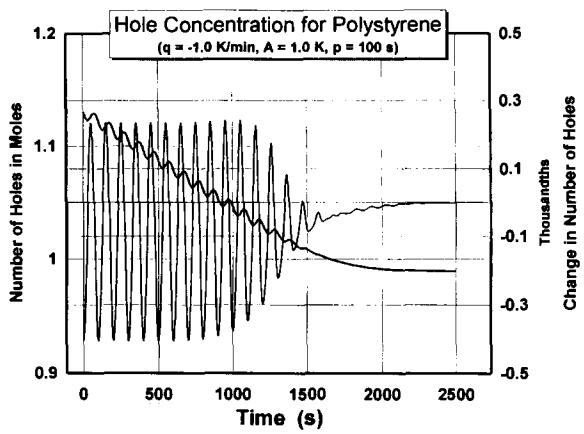

Fig. 2. Solution of the numerical integration of Eq. (6) on cooling, using the partial integration of Eq. (13). The heavier line refers to the number of holes, the thinner line to the change.

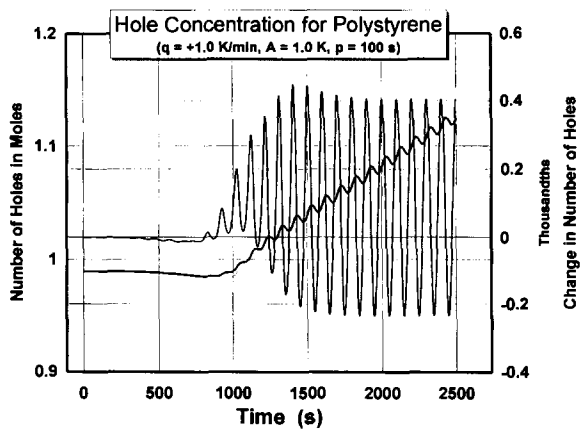

Fig. 3. Solution of the numerical integration of Eq. (6) on heating, using the partial integration of Eq. (13). The heavier line refers to the number of holes, the thinner line to the change.

experiment of Fig. 2, N_o is taken as the equilibrium value at T_o(=400.5 K, N_o=1.130225 mol). For the heating experiments, the initial N_o is the frozen number of holes observed on cooling as shown in Fig. 2 (T_o=358 K, N_o=0.98955 mol, the fictive temperature, T_f, the temperature where $N^*=N_o$, is 373.6 K). The glass transition is evident from the respective decreases and increases in modulation amplitudes.

The next step is to simulate the TMDSC experiment, assuming that all instrument lags have been minimized and steady state is maintained throughout the measurement, as described in detail in Refs. [9] and [10]. Figs. 4 and 5 are plots of the modulated heat flow [$HF(t)=\Delta N(t)\times\varepsilon_h$] and the smoothed, maximum amplitude of the pseudo-isothermal heat flow (smoothed $\langle A_{HF}\rangle$) in the bottom of the figures. The heat capacity, as measured in Fig. 1, is available from the smoothed $\langle A_{HF}\rangle$, as indicated in Eqs. (1)–(3). To find out the detailed characteristics of the kinetics, only non-smoothed heat capacities will be discussed below. The two top curves of Fig. 4 and Fig. 5 are the pseudo-isothermal cosine and sine components of the heat-flow amplitude [$A_{HF}\sin(\omega t-\delta)\cos\omega t$ (lower amplitudes) and $A_{HF}\sin(\omega t-\delta)\sin\omega t$ (upper amplitudes), respectively, with $A_{HF}\sin(\omega t-\delta)=HF(t)-\langle HF\rangle$]. They give on integration (averaging) over full modulation periods the Fourier components of modulation frequency

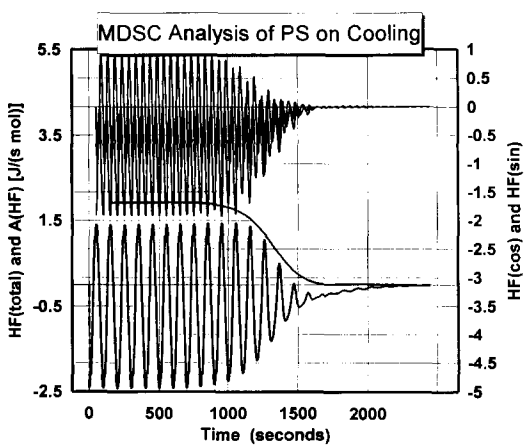

Fig. 4. Simulation of the software analysis of the heat flux on cooling, as given in Fig. 2. Spread sheet analysis as derived in Ref. [9]. Upper curves right ordinate, lower, left.

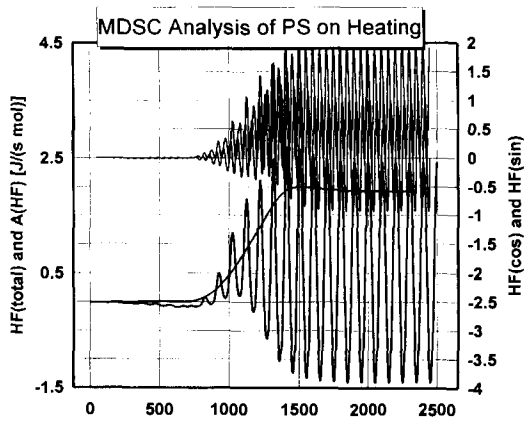

Fig. 5. Simulation of the software analysis of a heat flux on heating, as given in Fig. 3. Spread sheet analysis as derived in Ref. [9]. Upper curves right ordinate, lower, left.

ω of the reversing heat flow (first harmonic), and on vector addition, the pseudo-isothermal maximum modulation amplitude $\langle A_{HF}\rangle$ [9].

Figs. 6 and 7 illustrate the components of the heat capacity in the glass transition region without smoothing on cooling and heating as a function of the average temperature ($\langle T\rangle$, averaged over one modulation period). The total of this heat capacity is calculated from the heat-flow average ($\langle HF\rangle$, averaged over one modulation period without further smoothing). The reversing heat capacity is computed from Eq. (1), using the non-smoothed maximum amplitude $\langle A_{HF}\rangle$. The non-reversing heat capacity [C_p(irrev)] is the difference between the other two curves. Considerable periodic

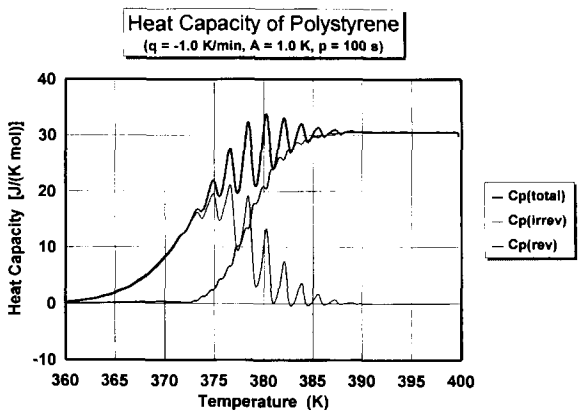

Fig. 6. Heat capacities on cooling, derived from Fig. 4.

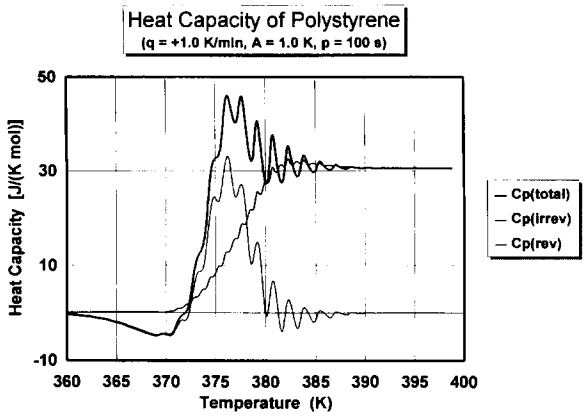

Fig. 7. Heat capacities on heating, derived from Fig. 5.

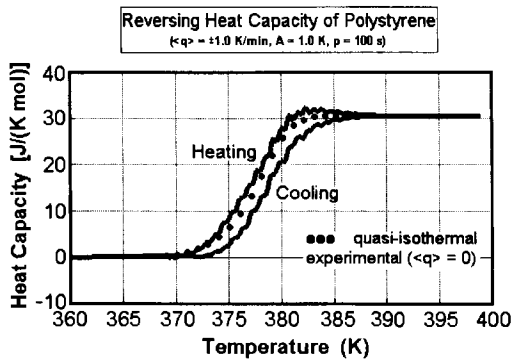

Fig. 8. Comparison of the reversing data of Figs. 6 and 7 with the quasi-isothermal experimental data of Fig. 1, normalized to the increase of heat capacity at the glass transition.

changes are seen in the total heat capacity in addition to the expected change for the glass transition. The frequency of these periodic changes can be estimated from the maxima between 375 and 385 K. The 10 K temperature difference is traversed in 300 s, i.e. within three modulation periods p of the sample temperature. In Fig. 6, on cooling, one finds that the periodic changes have been average repeat of about 106 s, while on heating, the repeat takes on average of 94 s. The enthalpy relaxation (hysteresis effect) on heating is seen in Fig. 7 in the total and nonreversing heat capacity curves. It consists of an exotherm between 360 and 372 K, followed by an endotherm, both superimposed with the periodic changes. The reversing heat capacity shows the shallower periodic changes of about half the repeating times (52 and 48 s, respectively). On smoothing, as in Figs. 4 and 5 the residual modulation effect disappears almost completely (see Figs. 4 and 5, smoothed $\langle A_{HF} \rangle$).

5. Discussion

5.1. Comparison of quasi-isothermal and pseudo-isothermal analysis of TMDSC

The reversing heat capacities of Figs. 6 and 7 are plotted in Fig. 8 together with the measured heat capacity, normalized to the increase in the glass transition region. The first observation is that the simulated curves differ from the quasi-isothermal experiments up to about ± 1 K, the same as seen in the experiments of Fig. 1. These deviations are less than typical variations for polystyrene from different origins. Because of the close correspondence with the quasi-isothermal data, the reversing component of the heat capacity can, thus, be used as a good estimate of the glass transition at the given modulation frequency. Even better is to use the average between heating and cooling runs at the same underlying rates $\langle q \rangle$, a value that is close to the quasi-isothermal measurement. The difference between heat capacities with and without underlying heating rate becomes negligible for small heating and cooling rates and low modulation amplitudes. The difference is less than 0.1 K at a $\langle q \rangle$ of 0.25 K min^{-1}, A of 0.1 K, and p=20 s.

5.2. Limits of the first-order kinetics

Looking at the finer details, one finds that only when the sample is close to the equilibrium liquid the simulation gives the correct apparent heat capacity (above about 380 K). Between 380 and 390 K the apparent heat capacity is nonlinear. On cooling it is lower than the quasi-isothermal analysis and on heating it is higher. To agree with the experimental data of Fig. 1 at lower temperatures, there must be a slower freezing than calculated on cooling, and a delay followed by a speed-up of the unfreezing on heating. Such effect is not contained in the glass transition kinetics of Eq. (6), irrespective of the assumed temperature dependence of N^* and τ. As usual for all

irreversible processes, close to equilibrium the simple first-order expression of Eq. (6) holds; further from equilibrium, however, it begins to deviate.

The analysis of glasses of different stability (thermal history) under identical MDSC conditions have also shown that the reversing heat capacity curves become sharper with higher stability of the initial sample (lower fictive temperature T_f). Fig. 9 illustrates this effect for a different polystyrene sample of lower glass transition temperature and lower activation energy measured earlier [4].

The asymmetry of the approach to equilibrium from states of higher and lower enthalpy (or volume) have been observed before [16]. Mathematically this "self-retarding" kinetics on approaching the final state by decreasing the number of holes and the "autocatalytic" kinetics on approaching the final state by increasing the number of holes is generally described by the Tool–Narayanaswamy–Moynihan equation [17]:

$$\tau = B \exp\left[\frac{x\varepsilon_j}{RT_o} + (1-x)\frac{\varepsilon_j}{RT_f}\right], \qquad (14)$$

where x is the nonlinearity parameter and T_f, the fictive temperature. The former can vary between zero and one. As x approaches one, the Arrhenius equation, Eq. (8), is recovered. As N approaches N^*, T_f becomes equal to T_o and Eq. (8) is recovered for all values of x. such change in the kinetics would also explain why the exotherm seen on computed heating curves for C_P (total) in Fig. 7 is much larger than seen in experiments [3]. Experiments on the relaxation of glasses of low volume and high enthalpy, formed on cooling at elevated pressure and analyzed at atmospheric pressure [18] showed, however, that volume and enthalpy relaxation follow a different kinetics, further complicating a full description of the glass transition.

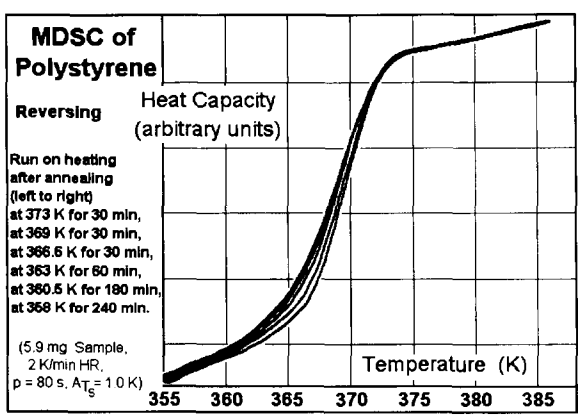

Fig. 9. Change of the reversing heat capacity measured on samples with different thermal history (decreasing stability, i.e. higher free enthalpy, for curves from left to right)[4].

It was also observed by cyclic dynamic differential thermal analysis (DDTA) [3] that the enthalpy relaxation occurs over a narrower temperature range than expected from Eq. (6) with an Arrhenius-type relaxation time τ. Such narrower, nonexponential temperature-range of relaxation excludes the introduction of a distribution of hole sizes to improve the fit between calculation and experiment, but suggests a cooperative process. To correct the analysis, the Arrhenius equation is usually replaced by the Kohlrausch–Williams–Watts stretched-exponential that raises the exponential of Eq. (8) to the power $\beta(0<\beta\leq 1)$. Final fittings has then been accomplished by introduction of a distribution of relaxation times. Even for only one relaxation time, such description needs three additional constants. Using assumed values, in a modeling approach similar to the one used in this research [19], Hutchinson could show, that indeed, the apparent heat capacities on heating and cooling cross [20]. Perhaps it is possible to extract the missing parameters from the frequency and heating rate dependence of the characteristic cross-over point in Fig. 1. All of these observations point to the necessity to develop a better, cooperative kinetics for the description of the glass transition. Quantitative data to guide such developments may become available through TMDSC.

5.3. *Modulation-effects on the reversing heat capacity*

A third observation that needs to be discussed is the origin of the remaining periodic changes of the total heat capacity seen in the calculated data of Figs. 6–8. They are not as obvious from Figs. 2–5 because of the prominent effect of the basic temperature modulation, and they cannot be seen in Fig. 1 because of the additional smoothing by the MDSC software. Their origin can be traced to the slight change in frequency in the modulated heat flow. The frequency decreases slightly on cooling relative to frequency of the temperature modulation, and increases on heating. In the time/temperature domain this may thought of as a

Doppler effect on the modulation frequency in the glass transition region. Ultimately, at sufficiently lower temperature, the heat flow changes to a more continuous drift towards N^* that becomes negligible below 360 K.

In the pseudo-isothermal data analysis, as simulated in Figs. 4–7[9], one extracts the fundamental, sinusoidal modulation of period p and, if present harmonics from the total heat flow for the determination of the reversing heat flow [by subtracting $\langle HF \rangle$ from $HF(t)$]. The component of frequency ω alone, the first harmonics, is reported as the reversing signal, as indicated in Figs. 4–7. Any oscillations of frequencies other than $n \times \omega$ (with n=any integer) are removed only partially when averaging $HF(t)$ over the period of the original modulation, p, to obtain $\langle HF \rangle$. The remaining parts of these other components in $\langle HF \rangle$ cause its periodic changes, seen best between 375 and 385 K in Figs. 6 and 7. Because of the slight frequency shift, relatively large changes with a period not far from p result. The total heat flow is in this temperature range obviously not equal to the one observed by standard DSC. The smoothing applied to the experimental data eliminates, however, most of the periodic changes so that the experimental output in Fig. 1 is only insignificantly different from standard DSC.

The even smaller periodic changes in the reversing heat capacity between 375 and 385 K have approximately double the frequency of the modulation and change less in amplitude over this temperature range (see Figs. 6 and 7). As pointed out above, part of the frequency-shifted response is assessed by the calculation of the reversing heat flow amplitude. Its sine and cosine components in Figs. 4 and 5 are affected differently, depending on the frequency difference and phase shift at any point of time. As a result, the observed periodic changes have approximately double the frequency, close to the frequency seen for HF(sin) and HF(cos). Again, the smoothing introduced for the final output of the MDSC software eliminates most of this effect since the periodic changes are rather symmetric (see Figs. 1, 4, 5).

For elimination of both effects and full information on the kinetics of the glass transition a complete Fourier analysis should be performed on $HF(t)$. It should be also be noted that our prior work [7,8] revealed that the glass transition kinetics introduces even for quasi-isothermal experiments a second harmonic frequency. This frequency should be part of a "reversible heat capacity". It is also important for the assessment of the kinetics in the glass transition and must be evaluated by determining the appropriate Fourier coefficients, either by a full transform, or in analogy to Figs. 4 and 5, from the components HF(cos 2ω) and $HF(\sin 2\omega)$ [9].

6. Conclusions

The glass transition can be studied as a function of frequency using TMDSC in the presence of a second time scale generated by the underlying heating rate $\langle q \rangle$. For highest precision, $\langle q \rangle$ should be low to approach the quasi-isothermal case, and the modulation amplitude should be small with relatively high frequency to separate the two time effects as much as possible. Improvements on the data can be made by averaging heating and cooling runs. The simple first-order kinetics model describes the changes of the pseudo-isothermal analysis quantitatively as long as the sample is close to equilibrium (the liquid state). The simple first-order kinetics of the glass transition with temperature and time dependent equilibrium numbers of high-energy configurations (holes, N^*) and relaxation time τ introduce a second harmonic of the modulation frequency and a phase shift in the glass transition region. The deviations of the calculations from the experiment at lower temperature can be understood qualitatively and points to the need to develop relaxation parameters that are dependent on the stability of the analyzed glass as expressed by its enthalpy, free enthalpy, or density and the cooperativity of the process. Existing mathematical expressions may be fitted to the data, but do not yet yield a detailed understanding of the molecular kinetics.

Acknowledgements

This work was supported by the Division of Materials Research, National Science Foundation, Polymers Program, Grant No. DMR 90-00520 and Oak Ridge National Laboratory, managed by Lockheed Martin Energy Research Corp. for the U.S. Department of Energy, under contract number DE-AC05-96OR22464. Some support came also from ICI Paints.

Also acknowledged are helpful discussions by the reviewers and attendies of the Fourth Lähnwitz Seminar, Krugsdorf, Germany, June 1996.

References

[1] M. Reading, Trends Polymer Sci. 8 (1993) 248.
[2] B. Wunderlich. Y. Jin and A. Boller, Thermochim. Acta 238 (1994) 277.
[3] B. Wunderlich, D.M. Bodily and M.H. Kaplan, J. Appl. Phys. 35 (1964) 95.
[4] A. Boller, C. Schick and B. Wunderlich, Proc. 23rd NATAS Conf., 1994. Full paper Thermochim. Acta, 266, 97 (1995).
[5] I. Okazaki and Bernhard Wunderlich, Proc. 11th Int. Conf. Thermal Anal. and Calorimetry (ICTAC), Philadelphia, PA, August 11–15, 1996. Full paper J. Polymer Sci., Polymer Phys., 34 (1996) 2941. .
[6] A. Boller, Y. Jin and B. Wunderlich, J. Thermal Analysis, 42 (1994) 307; see also Y. Jin, A. Boller, and B. Wunderlich, Proc. 22nd NATAS Conf., Denver, Sept. 19–22, K.R. Williams, ed., (1993) 59–64.
[7] B. Wunderlich, A. Boller, I. Okazaki and S. Kreitmeier, J. Thermal Anal. 47 (1996) 1013.
[8] A. Boller, I. Okazaki and B. Wunderlich, Thermochim. Acta, 284 (1996) 1; see also B. Wunderlich and A. Boller, Proc. 24th NATAS Conf., San Francisco, Sept. 10–13, S.A. Mikhail, ed., (1995) 136–141.
[9] B. Wunderlich, J. Thermal Analysis, in press, see also Proc. 11th Int. Conf. Thermal Anal. and Calorimetry (ICTAC) in Philadelphia, PA, August 11–15 (1996).
[10] B. Wunderlich, A. Boller, I. Okazaki and S. Kreitmeier, Thermochim. Acta, 282/283 (1996) 1430..
[11] D.A. Ditmars, S. Ishihara, S.S. Chang, G. Bernstein and E.D. West, J.S. Res. Natl. Bur. Stand. 87 (1982) 159.
[12] U. Gaur and B. Wunderlich, J. Phys. Chem. Ref. Data 11 (1982) 313.
[13] H. Eyring, Chem. Phys., 4, 238 (1936); J. Frenkel, Kinetic Theory of Liquids, Clarendon Press, Oxford, England (1946).
[14] N. Hirai and H. Eyring, J. Appl. Phys., 29 (1958) 810; J. Polymer Sci. 37 (1995) 51.
[15] I. Prigogine, Introduction to Thermodynamics in Irreversible Processes, Interscience, New York, NY (1961).
[16] A.J. Kovacs, Adv. Polymer Sci. 3 (1964) 394.
[17] S. Matsuoka, Relaxation Phenomena in Polymers, Hanser Verlag, Munich, Germany (1992).
[18] A. Weitz and B. Wunderlich, J. Polymer Sci., Polymer Phys., 12 (1974) 2473.
[19] J.M. Hutchinson, lecture at the Fourth Lähnwitz Seminar, Krugsdorf, Germany, June (1996), to be published (TMDSC in the Glass Transition Region).
[20] Communication and trial simulation by J.M. Hutchinson at the Fourth Lähnwitz Seminar, Krugsdorf, Germany, June (1996).